Mapping Retinal and Choroidal Thickness in Unilateral Nongranulomatous Acute Anterior Uveitis Using Three-Dimensional 1060-nm Optical Coherence Tomography

Maximilian Gabriel,[1] Robert Kruger,[1] Farnusch Shams-Mafi,[1] Boris Hermann,[2] Behrooz Zabihian,[2] Leopold Schmetterer,[2–6] Wolfgang Drexler,[2] Susanne Binder,[1] and Marieh Esmaeelpour[1,2]

[1]Karl Landsteiner Institute for Retinal Research and Imaging, Department of Ophthalmology, Rudolf Foundation Hospital, Vienna, Austria
[2]Center for Medical Physics and Biomedical Engineering, Medical University of Vienna, Vienna, Austria
[3]Singapore Eye Research Institute, Singapore National Eye Centre, Singapore
[4]Department of Ophthalmology, Lee Kong Chian School of Medicine, Nanyang Technological University, Singapore
[5]Ophthalmology and Visual Sciences Academic Clinical Program, Duke-NUS Medical School, Singapore
[6]Department of Clinical Pharmacology, Medical University of Vienna, Austria

Correspondence: Maximilian Gabriel, Department of Ophthalmology, Rudolf Foundation Hospital, Juchgasse 25, 1030 Vienna, Austria; max.gabriel@gmx.at.

Submitted: May 22, 2017
Accepted: August 22, 2017

Citation: Gabriel M, Kruger R, Shams-Mafi F, et al. Mapping retinal and choroidal thickness in unilateral nongranulomatous acute anterior uveitis using three-dimensional 1060-nm optical coherence tomography. *Invest Ophthalmol Vis Sci*. 2017;58:4778–4783. DOI:10.1167/iovs.17-22265

Purpose. To analyze retinal thickness (RT) and choroidal thickness (ChT) changes in patients with unilateral nongranulomatous acute anterior uveitis (AAU) using three-dimensional (3D) 1060-nm optical coherence tomography (OCT).

Methods. Retinal and choroidal thickness maps were statistically analyzed for 24 patients with newly diagnosed unilateral AAU before therapy. A total of 17 patients were followed until resolution of inflammatory activity (twice in the first week, then weekly). Resolution occurred in all subjects within 6 weeks after the initial diagnosis. After resolution, thickness maps were again generated. All patients were imaged by high-speed spectral-domain (SD) 3D 1060-nm OCT over a 10 × 10-mm field of view. The spatial distribution of retinal and choroidal thickness was mapped and analyzed using the Early Treatment Diabetic Retinopathy Study (ETDRS) grid.

Results. The choroid was significantly thicker in eyes affected by AAU than in fellow eyes before therapy with a mean thickness difference of 37 ± 11.44 µm (mean ± SD, Bonferroni correction, $\alpha = 0.0125$). Following therapy, ChT significantly decreased with a mean change of 24 ± 6.9 µm (mean ± SD, Bonferroni correction, $\alpha = 0.0125$). There was no significant difference in RT between AAU and fellow eyes before therapy or in AAU eyes before and after therapy.

Conclusions. Eyes affected by AAU demonstrate an increase in ChT before and a subsequent decrease after therapy while retinal thickness seems unaltered by disease and therapy. ChT might be a useful biomarker in monitoring posterior involvement and response to therapy in patients with AAU.

Keywords: choroidal thickness, acute anterior uveitis, optical coherence tomography

Nongranulomatous acute anterior uveitis (AAU) is the most frequent form of uveitis and most cases are due to idiopathic conditions.[1] Cystoid macular edema (CME) is often described as a potentially sight-threatening complication of AAU, but the pathogenesis of CME development is not fully understood and its prevalence varied considerably in different studies.[2–8] CME could either be a complication affecting only severe forms of AAU or be the endpoint in a spectrum of changes of the posterior segment in all forms of AAU, with the latter hypothesis suggesting that even mild forms of AAU could reveal changes in the posterior segment.

Advances in optical coherence tomography (OCT) have enabled choroidal imaging with longer imaging wavelengths, allowing good penetration at the retinal pigment epithelium (RPE) and visualization of the choroidal–scleral interface.[9,10]

Previous studies have revealed a typical choroidal thickness (ChT) pattern in various types of posterior uveitis such as Vogt-Koyanagi-Harada disease,[11] Behçet's disease,[12] sarcoidosis,[13] birdshot chorioretinopathy,[14] and sympathetic ophthalmia.[15] ChT generally increased during acute inflammation, decreased in response to therapy, and was thinner during remission when compared to healthy controls.

While ChT has been diligently investigated in posterior uveitis, little is currently known about potential posterior morphologic changes in AAU. One of two existing studies revealed differences in retinal thickness between the affected and the fellow eyes that became significant 7 days after disease onset and reached a maximum between 17 and 25 days (depending on the Early Treatment Diabetic Retinopathy Study [ETDRS] subfield).[16] The second study, an investigation by Gehl et al.,[17] found no difference in ChT between patients with AAU

or intermediate uveitis and healthy controls. That study, however, had some limitations. First, study and control eyes may not have been matched for axial eye length. Second, rather than measuring over a relevant field of view by averaging for every ETDRS subfield, the study relied on single scan measurements at three locations using enhanced-depth imaging optical coherence tomography (EDI-OCT). Measurement errors can be caused by a generally limited field of view for scanning and inconsistencies in finding the same location for repeated ChT measurements.[18]

In this investigation, retinal and ChT were compared to the healthy fellow eyes in 24 patients with unilateral AAU using both color-coded thickness maps and averaged thickness values for each subfield of the ETDRS grid. Overall, 17 patients were further followed until resolution of inflammatory activity in order to assess possible effects of conventional AAU therapy on layer thickness.

Methods

Study Population

A total of 24 newly diagnosed patients with AAU and no other history of ophthalmic disease were recruited. Approval was obtained from the Ethics Committee of the City of Vienna; the study adhered to the tenets of the Declaration of Helsinki, and informed consent forms were collected from all subjects before participation and after an introductory patient briefing. Exclusion criteria were previous episodes of AAU, diabetes, arterial hypertension, age-related macular degeneration, macular holes, epiretinal membranes, glaucoma, other retinal or choroidal diseases, CME, previous retinal treatment, and myopia or hypermetropia > 6 diopters.

Patients were recruited from the ophthalmologic outpatient clinic at the Rudolf Foundation Clinic in Vienna. In the course of the first visit, patients with untreated unilateral nongranulomatous AAU were included. Slit-lamp biomicroscopic examination was performed, arterial blood pressure was measured, and both intraocular pressure and visual acuity using the Snellen chart were assessed. Additionally, eye axial length was evaluated as a previous study reported a strong negative correlation between ChT and eye length.[19] The retinal status was evaluated using slit-lamp biomicroscopy with a Volk lens (Volk Optical, Inc., Mentor, OH, USA), and the severity of AAU was graded using the Standardization of Uveitis Nomenclature (SUN) classification.[20] Finally, the layer thickness was assessed using 1060-nm OCT. A total of 17 patients were subsequently followed (twice in the first week, then weekly) until resolution of inflammatory activity defined by the absence of both symptoms and cells or haze in the anterior chamber. Resolution occurred in all subjects within 6 weeks after the initial diagnosis. Patients were managed with hourly topical corticosteroid drops (prednisolone acetate 0.5%), topical corticosteroid ointment (prednisolone acetate 0.5%) in the evening, topical nonsteroidal anti-inflammatory drops (diclofenac natrium 1 mg/mL) four times/day, and topical anticholinergic drops (tropicamide 0.5%) two times/day. Therapy was adapted to inflammatory activity in subsequent follow-up visits. After resolution of inflammatory activity, slit-lamp biomicroscopy was again performed, both intraocular pressure and visual acuity were assessed, and layer thickness was recorded using 1060-nm OCT.

OCT Imaging

A 1060-nm spectral-domain OCT prototype previously described by Esmaeelpour et al.[19] and Povazay et al.[21] was used for this investigation. High-speed three-dimensional (3D) SD-OCT imaging was performed with a beam power of 2.5 mW at the cornea, well below the maximum power limit for 10 seconds of exposure. 3D OCT volumes were acquired at 1060 nm with 15- to 20-μm transverse resolution, approximately 7-μm axial resolution, and 512 voxels per depth scan (A-scan). Scans across a $36° \times 36°$ (10×10-mm) field at 60,000 A-scans per second were centered on the fovea and resulted in up to 120 frames per second. For image processing, ImageJ software was used (Wayne Rasband, National Institutes of Health, Bethesda, MD, USA), and Neat Image software (Neat Image; ABSoft, Troy, MI, USA) was utilized to reduce background noise. Automatic retinal and choroidal segmentation has been described elsewhere.[22] Briefly, this method determines the segmentation line in a low-signal, noisy environment such as OCT tomograms in the region of the choroid independent of boundary edge information. The resulting pixel distance is converted into optical distance using the depth sampling calibration for the 1060-nm OCT system and further to the anatomic distance. Automatic segmentation was controlled manually by an experienced observer who was masked to all clinical information. Axial retinal thickness (RT) was defined as the distance between the internal limiting membrane and the center of the peaks originating from the RPE/Bruch's membrane/choriocapillaris (RBC) complex and axial ChT as the distance between the RBC complex and the choroidal–scleral interface.

To investigate ChT variation throughout the entire field of view, ChT maps were generated based on automatic segmentation. The spatial distribution of retinal and choroidal thickness was analyzed using the ETDRS grid. The ETDRS grid divides the macula into nine subfields: the central, inner temporal, inner nasal, inner superior, inner inferior, outer temporal, outer nasal, outer superior, and outer inferior subfields. A total of 512 B-scans were recorded for each eye, of which 128 were segmented with 512 points of measurement each, resulting in 65,536 points per eye or 7282 points per ETDRS subfield. The paired *t*-test was used to compare both the eyes with AAU and the fellow eyes before therapy and the eyes with AAU before and after therapy. Following the recommendations of the section for Medical Statistics of the Medical University of Vienna, the layers were initially tested for significance without splitting into ETDRS subfields. For this step, the *P* value was adjusted according to the Bonferroni correction for repeated measures ($\alpha = 0.05/4 = 0.0125$). In a second step, layers that exhibited significant thickness change were further split into ETDRS subfields. The Bonferroni-Holm correction was used to adjust *P* values and therefore correct for multiple comparisons in this second step. The coefficient of repeatability, as defined by Bland and Altmann,[23] was previously calculated at 13.6 μm (Gabriel M, Esmaeelpour M, unpublished data, 2016).

Esmaeelpour et al.[24] have previously used an algorithm that offers good repeatability and reliability for automated analysis of choroidal vessel layer segmentation. They described a negative correlation between choroidal Haller's (outermost layer of the choroid consisting of larger-diameter blood vessels) and Sattler's layer (layer of medium-diameter choroidal blood vessels) thickness with age and axial length.[24] Another investigation by the same group demonstrated Haller's and Sattler's layer thinning in age-related macular degeneration (AMD).[25] We have experimentally tested this algorithm for our patient collective.

Averaging Group Measurements to Obtain Difference Maps

Difference maps were generated to spatially investigate changes in thickness by subtracting both grouped measure-

Table 1. Basic Patient Characteristics

Characteristics	*n*
Male patients	15
Female patients	9
Right eyes	16
Left eyes	8
SUN I	13
SUN II	7
SUN III	4
Complete follow-up	17
Remission within 1 wk	1
Remission between 1 and 3 wk	6
Remission between 3 and 6 wk	10
	Mean ± SD (Range)
Age	43 ± 11 (27–66)
Systolic blood pressure, mm Hg	124 ± 9 (110–145)
Diastolic blood pressure, mm Hg	83 ± 6 (75–100)
Intraocular pressure, mm Hg	15 ± 4 (9–20)
Axial length in study eyes, mm	24.03 ± 1.48 (21.06–27.99)
Axial length in contralateral eyes, mm	24.13 ± 1.53 (21.81–28.06)
BCVA in study eyes before treatment	0.9 ± 0.1 (0.5–1)
BCVA in study eyes in remission	1 ± 0.05 (0.9–1.1)
BCVA in contralateral eyes	1 ± 0.06 (0.8–1.1)

ments of the AAU eyes from the healthy fellow eyes before therapy and grouped measurements of the AAU eyes before therapy from the AAU eyes after therapy. This method of image analysis has been described in depth in a previous study.[19] ETDRS sublayer thickness was averaged and the grid was placed on the difference maps in order to illustrate areas of statistically significant thickness change.

Results

Demographic data are shown in Table 1. Fifteen male and 9 female subjects were included and there was a total of 16 right and 8 left eyes. Thirteen patients had grade 1 inflammation according to the SUN classification system and 10 of 17 patients who were followed until complete resolution of inflammatory activity went into remission between 3 and 6 weeks after disease onset.

The choroid was significantly thicker in the inflamed eyes than in the control eyes (Table 2) when all ETDRS subfields were analyzed (mean 37 ± 11.4 μm, Bonferroni correction, $\alpha = 0.0125$). Table 3 further illustrates this pattern using a subfield analysis based on the Bonferroni-Holm correction for multiple comparisons. The central subfield and four other subfields were significantly thickened in the inflamed eyes compared to the control eyes. Table 4 demonstrates that ChT decreased in response to therapy when all ETDRS subfields were analyzed, with a mean difference of 24 ± 6.9 μm (mean ± SD, Bonferroni correction, $\alpha = 0.0125$). A subfield analysis revealed significant differences in the central and the inner nasal subfield (Table 5). The Figure shows the previously introduced averaged thickness and difference maps for both the retina and the choroid to visually illustrate thickness differences in all patients. Pearson's coefficient showed no significant correlation between the severity of the inflammation at baseline based on the SUN classification and the difference in ChT between the inflamed and the healthy partner eyes at baseline ($P = 0.057$). There was no significant difference in RT and ChT between the healthy partner eyes at baseline or after remission and the AAU eyes after remission ($P > 0.05$). Differences in the mean ChT between the inflamed and the control eyes were highest in the inner temporal and lowest in the outer inferior subfield with an amplitude of 55 and 18 μm, respectively (Fig.). Differences in the mean ChT in the inflamed eyes before and after remission were highest in the inner nasal and lowest in the outer temporal subfield with an amplitude of 35 and 10 μm, respectively (Fig.). Similar to ChT, both Haller's and Sattler's layer responded to inflammation with an increase in

Table 3. Thickness Measurements of the Choroid at Baseline Using the ETDRS Grid, Mean ± SD (Range), and the Bonferroni-Holm (B-H) Correction

Subfields	Mean ChT, μm	*P* Value	*P* Value, B-H	α, B-H
Central				
AAU	330 ± 101 (120–538)	0.0004	0.003	0.0063
Control	282 ± 81 (138–423)			
Inner superior				
AAU	321 ± 86 (153–473)	0.007	0.026	0.0125
Control	287 ± 78 (140–443)			
Inner nasal				
AAU	311 ± 88 (150–461)	0.0009	0.005	0.01
Control	273 ± 80 (144–397)			
Inner inferior				
AAU	320 ± 95 (110–500)	0.0008	0.005	0.008
Control	279 ± 79 (119–422)			
Inner temporal				
AAU	320 ± 104 (106–538)	0.0002	0.002	0.0056
Control	265 ± 83 (105–416)			
Outer superior				
AAU	292 ± 61 (121–399)	0.048	0.096	0.025
Control	263 ± 80 (77–402)			
Outer nasal				
AAU	248 ± 78 (84–383)	0.018	0.055	0.0167
Control	223 ± 73 (135–374)			
Outer inferior				
AAU	287 ± 96 (89–435)	0.12	0.12	0.05
Control	269 ± 80 (92–401)			
Outer temporal				
AAU	285 ± 91 (77–435)	0.0004	0.003	0.007
Control	243 ± 79 (71–361)			

Table 2. Thickness Measurements of the Retina and the Choroid at Baseline, Mean ± SD (Range), and the Bonferroni Correction ($\alpha = 0.0125$)

All subfields	Mean RT, μm	*P* Value	Mean ChT, μm	*P* Value
AAU	292 ± 36 (120–370)	0.1	302 ± 92 (77–538)	<0.00001
Control	292 ± 33 (128–362)		265 ± 80 (71–443)	

Table 4. Thickness Measurements of the Retina and the Choroid Before and After Remission, Mean ± SD (Range), and the Bonferroni Correction ($\alpha = 0.0125$)

All subfields	Mean RT, μm	*P* Value	Mean ChT, μm	*P* Value
AAU	292 ± 35 (178–360)	0.75	282 ± 90 (77–473)	<0.00001
Remission	292 ± 38 (163–375)		258 ± 86 (60–455)	

Table 5. Thickness Measurements of the Choroid Before and After Remission Using the ETDRS Grid, Mean ± SD (Range), and the Bonferroni-Holm Correction

Subfields	Mean ChT, µm	*P* Value	*P* Value, B-H	α, B-H
Central				
AAU	305 ± 97 (120–462)	0.0005	0.004	0.0063
Remission	275 ± 87 (125–440)			
Inner superior				
AAU	304 ± 86 (153–473)	0.0036	0.025	0.007
Remission	281 ± 81 (152–418)			
Inner nasal				
AAU	295 ± 90 (150–451)	0.0001	0.001	0.0056
Remission	260 ± 82 (154–408)			
Inner inferior				
AAU	295 ± 92 (110–441)	0.15	0.6	0.0125
Remission	275 ± 93 (111–430)			
Inner temporal				
AAU	294 ± 100 (106–471)	0.053	0.26	0.01
Remission	272 ± 90 (109–455)			
Outer superior				
AAU	266 ± 82 (119–399)	0.2	0.6	0.0167
Remission	240 ± 88 (60–367)			
Outer nasal				
AAU	241 ± 85 (84–383)	0.02	0.1	0.008
Remission	213 ± 76 (122–367)			
Outer inferior				
AAU	275 ± 88 (117–435)	0.3	0.66	0.025
Remission	254 ± 92 (105–434)			
Outer temporal				
AAU	265 ± 91 (77–432)	0.5	0.5	0.05
Remission	255 ± 83 (84–423)			

thickness compared to the healthy partner eyes. Following therapy, thickness values decreased to baseline levels. In our investigation, however, there was a significant amount of noise in Haller's and Sattler's layer measurements.

Discussion

The prevalence of severe complications of acute AAU such as vitritis, papillitis, retinal vasculitis, epiretinal membranes, or CME varied considerably in different studies.[2–7] Subclinical retinal thickening, as a less severe form of posterior involvement, was observed in a study by Balaskas et al.[16] The authors revealed differences in RT between human leukocyte antigen (HLA) B27-positive eyes with AAU and healthy fellow eyes that became significant 7 days after disease onset and reached a maximum between 17 and 25 days (depending on the ETDRS subfield) with all subjects affected at this time point.[16]

Currently, little is known about subclinical ChT changes in AAU. An investigation by Gehl et al.[17] found no difference in ChT between patients with AAU or intermediate uveitis and healthy controls. That study relied on single scan measurements at three locations using EDI-OCT. EDI-OCT utilizes a wavelength not suited to measuring thick choroids.[19] Other limitations of this study were mentioned in the introductory part of this manuscript.

Unlike the retina with the fovea as its natural center, single-location imaging of the choroid appears unfeasible given its diverse topography. It has caused notable disparity between ChT measurements obtained in different studies. Discrepancies are caused by a generally limited field of view for scanning and inconsistencies in choosing the exact locations for repeated ChT measurements.[18] The inability to average ChT measurements further reduces the reliability of single-location imaging.

Esmaeelpour et al.[19] have previously published ChT maps in normal subjects and improved posterior segment visualization in cataract patients using 1060-nm OCT. Although OCT systems centered at 800 nm can resolve all major intraretinal layers, they enable only limited penetration beyond the retina due to multiple scattering and absorption in the melanin-rich RPE. This results in limited visualization of the choroid. Moreover, in clinical OCT, turbid ocular media (such as cataract or corneal haze) represent a significant challenge when imaging the retina.[26] Using a wavelength range around 1060 nm, where water absorption from the vitreous has a local minimum, the melanin in the RPE no longer inhibits the imaging of the choroid.[27]

In our investigation, the choroid may have responded to inflammation with an increase in thickness compared to the healthy partner eye. Following therapy, ChT decreased to baseline levels. Previous studies have revealed a similar ChT pattern in various types of posterior uveitis[11–15]: ChT generally increased during acute inflammation, decreased in response to therapy, and was thinner during remission when compared to healthy controls. Retinal thickness, on the other hand, was altered neither at baseline nor after treatment in our study. This could be due to the fact that HLA-B27 positivity was not tested in our study but was among the inclusion criteria of the aforementioned investigation by Balaskas et al.[16]

Various risk factors for CME have been described by Van Kooij et al.,[5] among them age, papillary leakage, mean body mass index, mean pack-years (smoking), and the location of uveitis: Posterior uveitis and panuveitis were both significantly associated with CME, while anterior uveitis and intermediate uveitis were not. However, only seven patients with anterior uveitis were tested. In another study by Dodds et al.,[2] 7 of 114 patients with HLA-B27–positive AAU developed CME.[2] CME could therefore either be a complication affecting only severe forms of AAU or be the endpoint in a spectrum of changes of the posterior segment in all forms of AAU. Our data indicate that the latter hypothesis may be true because all eyes with AAU showed choroidal thickening. This would mean that AAU is a disease generally affecting both the anterior and posterior segments, with the anterior segment being the main focal point in common cases.

Both the iris and the ciliary body have associations with the choroid in terms of blood supply. The blood for the iris and the ciliary body is provided by the anterior ciliary arteries, the long posterior ciliary arteries, and some anastomotic channels from the anterior choroid. The choroid is supplied by the short posterior ciliary arteries. The venous drainage of both iris and ciliary body and the choroid is conducted by the vortex veins.[28] We conclude that there are associations between the anterior and posterior uvea in terms of blood supply and drainage, although the blood supply is obviously not identical. Inflammatory mediators primarily effective in the anterior segment could likely spread to the posterior segment and cause choroidal thickening. Also, increased hydrostatic pressure levels in the anterior uvea could cause choroidal thickening by transmitting the increased pressure to the choroid.

There are some limitations to this study. First, HLA-B27 positivity is associated with a higher prevalence for posterior complications in AAU, but was not tested in our investigation. Second, a long-term follow-up visit would have been useful in order to determine possible choroidal thinning during disease

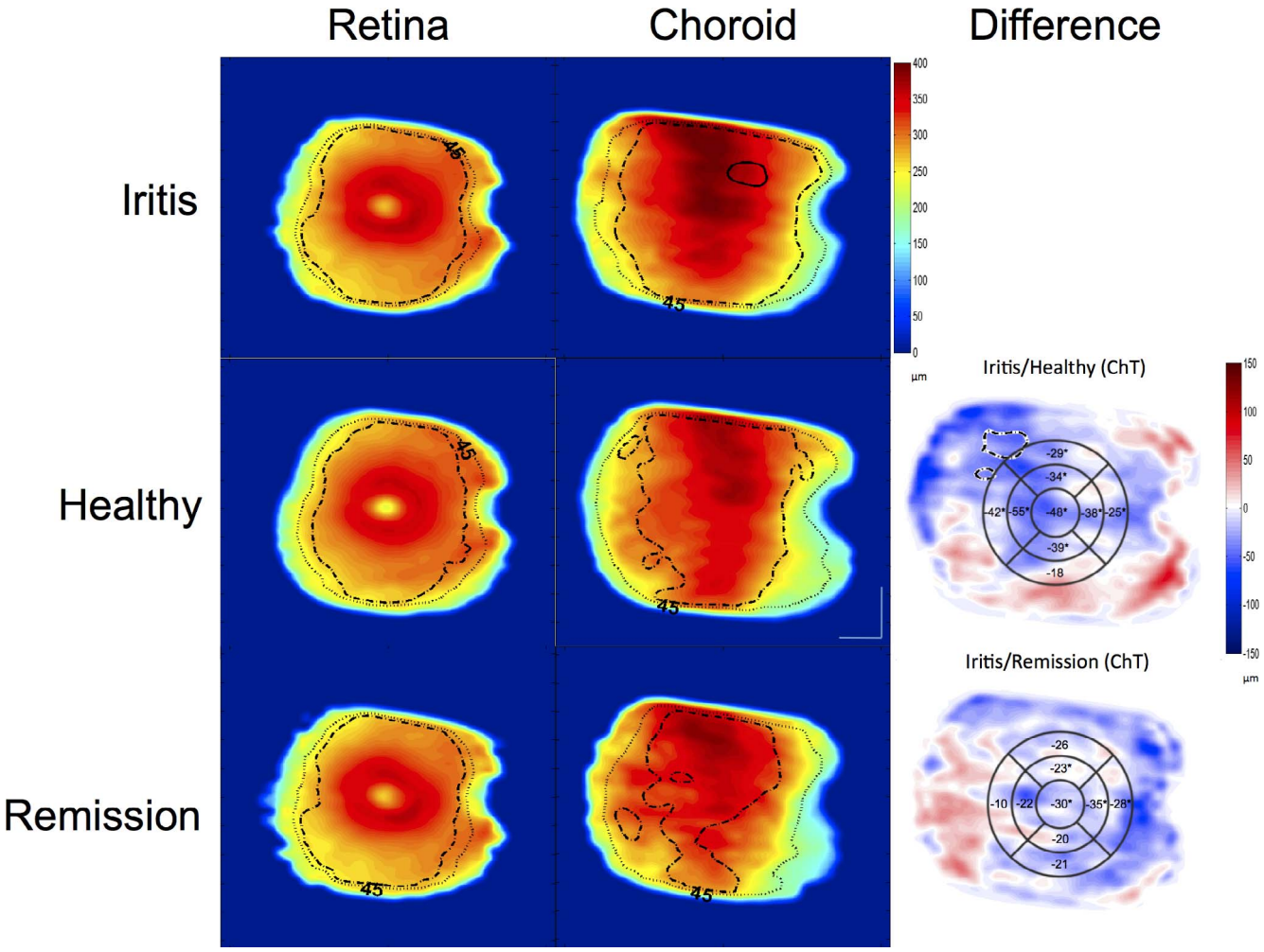

Figure. Averaged and difference maps for the retina and the choroid. Retinal thickness showed no variation, while the choroid was thicker in the eyes with AAU than in the healthy control eyes and in the AAU eyes after remission.

remission as has been observed in various types of posterior uveitis. Furthermore, it remains unclear if ChT decrease is a consequence of eye drop therapy or of resolution of inflammatory activity because no patients were followed after eye drop therapy was stopped. Follow-up studies are required to investigate choroidal sublayer thickness variation. ChT change can be triggered by different factors such as alterations in vessel diameter, inflammation, or fibrosis. Clearly, these factors are different in nature but can cause ChT changes that appear identical when ChT is measured exclusively. Future studies should aim to highlight these factors using techniques such as choroidal vessel layer segmentation.

In conclusion, we have demonstrated choroidal thickening in patients with AAU compared to healthy partner eyes. Clinical complications of AAU such as CME could represent serious endpoints in a spectrum of changes in the posterior segment that may begin with ChT alterations. This could indicate a paradigm shift because AAU was previously regarded as a disease of the anterior segment only.

Acknowledgments

Supported by Oesterreichische Nationalbank (Jubilaeumsfond, Project 14294).

Disclosure: **M. Gabriel**, None; **R. Kruger**, None; **F. Shams-Mafi**, None; **B. Hermann**, None; **B. Zabihian**, None; **L. Schmetterer**, None; **W. Drexler**, Carl Zeiss Meditec (C); **S. Binder**, Carl Zeiss Meditec (C); **M. Esmaeelpour**, Bayer (E)

References

1. McCannel CA, Holland GN, Helm CJ, Cornell PJ, Winston JV, Rimmer TG; for the UCLA Community-Based Uveitis Study Group. Causes of uveitis in the general practice of ophthalmology. *Am J Ophthalmol*. 1996;121:35–46.
2. Dodds EM, Lowder CY, Meisler DM. Posterior segment inflammation in HLA-B27+ acute anterior uveitis: clinical characteristics. *Ocul Immunol Inflamm*. 1999;7:85–92.
3. D'Ambrosio EM, La Cava M, Tortorella P, Gharbiya M, Campanella M, Iannetti L. Clinical features and complications of the HLA-B27-associated acute anterior uveitis: a metanalysis. *Semin Ophthalmol*. 2016:1–13.
4. Rodriguez A, Akova YA, Pedroza-Seres M, Foster CS. Posterior segment ocular manifestations in patients with HLA-B27-associated uveitis. *Ophthalmology*. 1994;101:1267–1274.
5. van Kooij B, Probst K, Fijnheer R, Roest M, de Loos W, Rothova A. Risk factors for cystoid macular oedema in patients with uveitis. *Eye (Lond)*. 2008;22:256–260.
6. Uy HS, Christen WG, Foster CS. HLA-B27-associated uveitis and cystoid macular edema. *Ocul Immunol Inflamm*. 2001;9:177–183.

7. Kim SJ, Chung H, Yu HG. Posterior segment involvement in Korean patients with HLA-B27-associated uveitis. *Ocul Immunol Inflamm*. 2009;17:26–32.
8. Fardeau C, Champion E, Massamba N, LeHoang P. Uveitic macular edema. *Eye (Lond)*. 2016;30:1277–1292.
9. de Boer JF, Cense B, Park BH, Pierce MC, Tearney GJ, Bouma BE. Improved signal-to-noise ratio in spectral-domain compared with time-domain optical coherence tomography. *Optics Lett*. 2003;28:2067–2069.
10. Unterhuber A, Povazay B, Hermann B, Sattmann H, Chavez-Pirson A, Drexler W. In vivo retinal optical coherence tomography at 1040 nm - enhanced penetration into the choroid. *Opt Express*. 2005;13:3252–3258.
11. Maruko I, Iida T, Sugano Y, et al. Subfoveal choroidal thickness after treatment of Vogt-Koyanagi-Harada disease. *Retina*. 2011;31:510–517.
12. Kim M, Kim H, Kwon HJ, Kim SS, Koh HJ, Lee SC. Choroidal thickness in Behcet's uveitis: an enhanced depth imaging-optical coherence tomography and its association with angiographic changes. *Invest Ophthalmol Vis Sci*. 2013;54:6033–6039.
13. Gungor SG, Akkoyun I, Reyhan NH, Yesilirmak N, Yilmaz G. Choroidal thickness in ocular sarcoidosis during quiescent phase using enhanced depth imaging optical coherence tomography. *Ocul Immunol Inflamm*. 2014;22:287–293.
14. Keane PA, Allie M, Turner SJ, et al. Characterization of birdshot chorioretinopathy using extramacular enhanced depth optical coherence tomography. *JAMA Ophthalmol*. 2013;131:341–350.
15. Fleischman D, Say EA, Wright JD, Landers MB. Multimodality diagnostic imaging in a case of sympathetic ophthalmia. *Ocul Immunol Inflamm*. 2012;20:300–302.
16. Balaskas K, Ballabeni P, Guex-Crosier Y. Retinal thickening in HLA-B27-associated acute anterior uveitis: evolution with time and association with severity of inflammatory activity. *Invest Ophthalmol Vis Sci*. 2012;53:6171–6177.
17. Gehl Z, Kulcsar K, Kiss HJ, Nemeth J, Maneschg OA, Resch MD. Retinal and choroidal thickness measurements using spectral domain optical coherence tomography in anterior and intermediate uveitis. *BMC Ophthalmol*. 2014;14:103.
18. Ouyang Y, Heussen FM, Mokwa N, et al. Spatial distribution of posterior pole choroidal thickness by spectral domain optical coherence tomography. *Invest Ophthalmol Vis Sci*. 2011;52:7019–7026.
19. Esmaeelpour M, Povazay B, Hermann B, et al. Three-dimensional 1060-nm OCT: choroidal thickness maps in normal subjects and improved posterior segment visualization in cataract patients. *Invest Ophthalmol Vis Sci*. 2010;51:5260–5266.
20. Jabs DA, Nussenblatt RB, Rosenbaum JT. Standardization of uveitis nomenclature for reporting clinical data. Results of the First International Workshop. *Am J Ophthalmol*. 2005;140:509–516.
21. Povazay B, Hermann B, Hofer B, et al. Wide-field optical coherence tomography of the choroid in vivo. *Invest Ophthalmol Vis Sci*. 2009;50:1856–1863.
22. Kajic V, Esmaeelpour M, Povazay B, Marshall D, Rosin PL, Drexler W. Automated choroidal segmentation of 1060 nm OCT in healthy and pathologic eyes using a statistical model. *Biomed Opt Express*. 2012;3:86–103.
23. Bland JM, Altman DG. Measurement error. *BMJ*. 1996;313:744.
24. Esmaeelpour M, Kajic V, Zabihian B, et al. Choroidal Haller's and Sattler's layer thickness measurement using 3-dimensional 1060-nm optical coherence tomography. *PLoS One*. 2014;9:e99690.
25. Esmaeelpour M, Ansari-Shahrezaei S, Glittenberg C, et al. Choroid, Haller's, and Sattler's layer thickness in intermediate age-related macular degeneration with and without fellow neovascular eyes. *Invest Ophthalmol Vis Sci*. 2014;55:5074–5080.
26. Besharse JC, Bok D. *The Retina and Its Disorders*. Academic Press; 2011.
27. Esmaeelpour M, Brunner S, Ansari-Shahrezaei S, et al. Choroidal thinning in diabetes type 1 detected by 3-dimensional 1060 nm optical coherence tomography. *Invest Ophthalmol Vis Sci*. 2012;53:6803–6809.
28. Kiel JW. Anatomy. *The Ocular Circulation*. San Rafael, CA: Morgan & Claypool Life Sciences; 2010.

Investigative Ophthalmology & Visual Science